Interpreting the Dynamic Association of Nanoplastics with Chlorella vulgaris: Insight from Single-cell Analysis and Gaussian Mixture Modelling

Rega Permana[1,2*], Swati Sharma[1], Bashiru Ibrahim[1,3], Tajudeen A. Oyehan[1], Christopher Stark[1], Miguel Gomez-Gonzalez[4], Christian Pfrang[1], Eugenia Valsami-Jones[1*]

[1]*School of Geography, Earth and Environmental Sciences, University of Birmingham, Birmingham, Edgbaston, B15 2TT, United Kingdom*

[2]*Faculty of Fisheries and Marine Science, Universitas Padjadjaran, Jatinangor, Sumedang, 45363, Indonesia*

[3]*Department of Biochemistry and Molecular Biology, Faculty of Sciences, Sokoto State University, Sokoto State, 852101, Nigeria*

[4]*Diamond Light Source, Harwell Science and Innovation Campus, Didcot OX11 0DE, United Kingdom*

**Corresponding author: rxp286@student.bham.ac.uk, e.valsamijones@bham.ac.uk*

Text S1. Eu-doped NPls Synthesis

Europium-doped polystyrene nanoplastics (Eu-doped NPls) were synthesized via emulsion polymerization based on our previous protocol. Monomer, initiator, and stabilizer were added to 18.75 mL deionized water in a three-neck flask equipped with a reflux condenser and nitrogen gas inlet, placed in an oil bath. The mixture was stirred at 150 rpm, heated to 70 °C over 30 minutes, and maintained at this temperature for 3 hours. In parallel, europium salt (0.01 wt%) and AAEM (8 wt%) were dissolved in another 18.75 mL of deionized water, preheated to 70 °C for 30 minutes, and then introduced into the main mixture. The reaction proceeded under constant nitrogen flow to prevent oxygen inhibition and was maintained at 70 °C for a total of 3 h.

Text S2. Growth rate estimation and inhibition rate (IR) analysis

The growth rate of *C. vulgaris* was estimated using a first-order nonlinear kinetic model [1]. This approach involved fitting the temporal changes in cell density to the model, thereby determining the growth rate constant and providing insights into the exponential proliferation dynamics of the algae under the experimental conditions. The model can be calculated using the following formula:

$$N_t = N_0(e^{-\mu t})$$

where N_t and N_0 are the cell density of *C. vulgaris* (cells/mL) at time t and 0, respectively, and μ is the growth rate constant (per h).

The growth inhibition rate (IR) was determined by comparing the cell densities in each exposure group with an untreated group (control). This metric quantifies the reduction in cell growth due to Eu-doped NPls exposure and was calculated using the formula described below [2].

$$IR = \frac{C_c - C_t}{C_c}$$

Where, C_c and C_t are the cell density of the control and treatment groups, respectively.

Text S3. Sample digestion

A total acid digestion was performed to completely dissolve organic matrix of the concentrated microalgae cells upon growth inhibition test. Briefly, a mixture of 8:1 HNO_3 and H_2SO_4 was added to the sample followed by addition H_2O_2 for full organic matter breakdown. To complete the digestion process, heat (80°C) was applied to the mixture until a clear solution was obtained, signifying the complete destruction of organic material. The final clear solution was then diluted 10 times with 2% HNO_3 prior to ICP-MS measurement.

Text S4. Estimation of SC-ICP-MS limit of detection (LOD)

Eu events were identified using a 3σ threshold above the background signal, corresponding to an instrumental threshold of 1.01 counts per dwell under the acquisition conditions used in this study. This threshold was applied to distinguish transient Eu events from baseline noise.

The mass-equivalent limit of detection (LOD) for Eu was estimated using the calibration-based approach [3]:

$$LOD = \frac{3.3 \times SD_{blank}}{\text{slope}}$$

where SD_{blank} is the standard deviation of the blank signal and *slope* is the sensitivity obtained from the Eu calibration. Following this approach, consistent with the framework described for single-cell/single-particle ICP-MS data treatment by Meyer et al. [3], the Eu detection limit was estimated to be approximately 45 ag per event under the applied SC-ICP-MS conditions.

Text S5. Modelling subpopulation using GMM

To investigate the heterogeneity of Eu-doped NPls across individual cells, we modelled the Eu mass per cell as a finite mixture of normal distributions using a Gaussian Mixture Model (GMM). Raw frequency data were expanded into a vector of individual Eu mass observations.

Each observation (x) was assumed to be generated from a mixture of *K* Gaussian components:

$$f(x|\theta) = \sum_{i=1}^{k} \gamma_i \, . \, \phi(x|\mu_i, \sigma_i^2)$$

where:

λ_i is the mixing weight for the i-th component ($\sum\lambda_i = 1$),

$\phi(x|\mu_i, \sigma_i^2)$ is the probability density function of the normal distribution with mean μ_i and variance σ_i^2,

$\theta = \{\lambda_i \mu_i, \sigma_i^2\}_{i=1}^{k}$ is the set of all parameters.

Model parameters were estimated via the Expectation-Maximization (EM) algorithm, implemented using the mixtools package in R. In each iteration, E-step and M-step was applied following the equation [4]:

E-step: Compute posterior probabilities γ_{jk}, the probability that observation x_j comes from component K:

$$\gamma_{jk} = \frac{\gamma_k . \phi(x_j|\mu_k, \sigma_k^2)}{\sum_{l=1}^{K} \lambda_1 . \phi(x_j|\mu_l, \sigma_l^2)}$$

M-step: Update model parameters:

$$\gamma_k^{new} = \frac{1}{n} \sum_{j=1}^{n} \gamma_{jk}$$

$$\mu_k^{new} = \frac{\sum_{j=1}^{n} \gamma_{jk} \, x_j}{\sum_{j=1}^{n} \gamma_{jk}}$$

$$\sigma_k^{2\,new} = \frac{\sum_{j=1}^{n} \gamma_{jk} \left(x_j - \mu_k^{new}\right)^2}{\sum_{j=1}^{n} \gamma_{jk}}$$

GMM model evaluation metric

Model Selection: BIC

We fitted models with K=1 to 6 components and evaluated their fit using the Bayesian Information Criterion (BIC):

Log-likelihood (ℓ) was computed as:

$$\ell(\theta) = \sum_{j=1}^{n} log\left[\sum_{i=1}^{K} \phi(x|\mu_i, \sigma_i^2)\right]$$

Number of free parameters:

$$p = (K-1) + K + K = 3K - 1$$

Where:

K – 1 mixing weights (since $\sum \lambda_i = 1$)

K means μ_i

K variances σ_i^2

Bayesian Information Criterion (BIC)

$$BIC = \log(n)\,.p - 2\ell(\theta)$$

Mean Absolute Error (MAE):

$$MAE = \frac{1}{n}\sum_{i=1}^{n}|Y_i' - Y_i|$$

Root Mean Squared Error (RMSE):

$$RMSE = \sqrt{\frac{1}{n}\sum_{i=1}^{n}(Y_i' - Y_i)^2}$$

Pearson correlation coefficient (ρ):

$$\rho = \frac{cov(Y, Y')}{\sqrt{Var(Y).Var(Y')}}$$

where Y is the observed frequency distribution and Y' is the predicted density from the GMM.

Text S6. Modelling interaction of Growth Inhibition and subpopulation using GLM

To quantify how specific Eu-doped NPls-loaded subpopulations modulate growth inhibition, a reduced GLM was fitted that contains only one pair of clusters (subpopulation) variables at a time together with the external exposure factors (dose and time). The analysis focused on the statistically and biologically most informative pairwise reduced models. For a given cluster pair *a–b* (e.g., cluster 1 + cluster 3, etc.) the multivariate analysis was denoted according to the previous study with modification [5]:

$$\hat{Y} = \beta_0 + \beta_1 Dose + \beta_2 Time + \beta_3 C_a + \beta_4 C_b + \varepsilon,$$

where:

$\hat{Y}$ = predicted growth-inhibition (%) of *C. vulgaris*,

Dose = nominal NPl concentration (mg/L),

Time = exposure duration (h),

C_a and C_b = fractions of cells in cluster *a* and cluster *b* (0–1),

$\beta_{0..4}$ = regression coefficients estimated by maximum likelihood,

$\varepsilon \sim N(0,\sigma^2)$ = the Gaussian error term.

Model adequacy was confirmed by AIC, RMSE, and McFadden/Nagelkerke pseudo-R^2 with R packages. Confidence intervals (95 %) for β were obtained from the profile likelihood.

GLM Evaluation Criteria

Model quality and performance were evaluated using the following criteria:

Akaike Information Criterion (AIC):

$$AIC = 2k - 2\ln(\hat{L})$$

Where:

- k: Number of estimated parameters
- $\hat{L}$: Maximum likelihood of the fitted model

A lower AIC indicates a better balance between goodness-of-fit and model complexity.

Root Mean Squared Error (RMSE):

$$RMSE = \sqrt{\frac{1}{n}\sum_{i=1}^{n}(y_i - \hat{y}_i)^2}$$

Where:

- y_i: Observed inhibition
- $\hat{y}_i$: Predicted inhibition
- n: Number of observations

Pseudo-R^2 values were used to assess model explanatory power

McFadden's R^2:

$$R^2_{McF} = 1 - \frac{lnL_{model}}{lnL_{null}}$$

Nagelkerke's R^2:

$$R^2_{Nag} = \frac{R^2_{McF}}{1 - \exp\left(\frac{2}{n} lnL_{null}\right)}$$

Where:

- lnL_{model}: Log-likelihood of the fitted model
- lnL_{null}: Log-likelihood of a null (intercept-only) model

Text S7. Determination of Chlorophyll a

Chlorophyll-a (Chl-a) determination was performed following previously described protocols [6]. In summary, 10 mL of microalgal culture from each treatment was withdrawn from the experimental flasks at 24, 48, and 72 h and centrifuged at 3600 g for 10 min. The supernatant was decanted, and the pellet was retained for further processing. An equal volume of 90% methanol (Fischer, UK) was added to the pellet, and the mixture was vigorously shaken before being incubated in a water bath at 60 °C for approximately 30 min. The samples were then allowed to cool to room temperature in the dark for 10 mins, followed by a second centrifugation at 3600 g for 10 mins. The Chl-a content was determined spectrophotometrically by measuring the absorbance of the supernatant at 665 and 652 nm, and the results were evaluated using the following equation [6]:

$$Chlorophyll\ a\ (mg/L) = 16.82A_{665} - 9.28A_{652}$$

Text S8. Determination of CO_2 uptake rate

The CO_2 fixation rate was determined using previously described method [7]. In brief, two subsamples were obtained from each treatment at the end of the 72-h exposure test. The first subsample was used for dry weight calculation; a known volume of culture was dried at 70 °C for 24 h and then weighed. The second subsample was centrifuged at 3600 g for 10 min and thoroughly washed with 10× PBS. The washed cells were subsequently lyophilized at –55 °C for 72 h, and the dried cells were analyzed for carbon content using an CE-440 elemental analyzer (Exeter analytical Inc., UK). The CO_2 fixation rate was then calculated using the following equation:

$$CO_2\ fixation\ rate = P \times C\ M_{CO_2} \times M_C$$

where P ($g_{biomass}$/L/d) is the biomass productivity; C (w/w) is the carbon content from elemental analysis and M_{CO_2} and M_C (g/mol) is the molar mass of CO_2 and C, respectively.

Text S9. ROS determination

Intracellular reactive oxygen species (ROS) were assessed using the fluorescent dye 2′,7′-dichlorodihydrofluorescein diacetate (H_2DCFDA; Sigma Aldrich, USA) according to previously described method [8]. A 10 mM stock solution of H_2DCFDA was prepared in deionized water and stored in the dark at –20 °C. The assay was performed at 24, 48, and 72 hours of exposure for each treatment. At each time point, 0.1 mL of culture was transferred to

a 96-well plate, and an equal volume of 0.2 mM H_2DCFDA was subsequently added. The mixture was gently shaken and incubated in the dark at room temperature for 30 minutes. At least five replicates were prepared for each treatment, and fluorescence intensity was recorded using a multi-plate reader (Tecan spark, Switzerland) with an excitation wavelength of 485 nm and an emission wavelength of 535 nm.

Text S10. Lipid Peroxidation assay (MDA)

Lipid peroxidation was determined by measuring malondialdehyde (MDA) equivalents at 24, 48, and 72 hours, according to a previously described method [9, 10]. In brief, a known volume of culture at a cell density of 10^6 cells/mL was collected from each treatment. The samples were centrifuged at 4,000 g for 10 minutes to obtain cell pellets. After decanting the supernatant, 5 mL of 0.1% trichloroacetic acid (TCA) was added, and the mixture was sonicated for 60 seconds using a W-220F sonicator (with 30-second pulses separated by 15-second intervals). The sonicated mixture was then combined with 5 mL of 0.5% thiobarbituric acid (TBA) in 20% TCA solution and incubated in a water bath at 95 °C for 30 minutes. After cooling to room temperature, the samples were centrifuged at 10,000 g for 10 minutes, and the absorbance of the supernatant was measured spectrophotometrically at 532 nm and 600 nm (to correct for background interference). Using a molar absorption coefficient ($\varepsilon = 1.5 \times 10^5$ M^{-1} cm^{-1}), the concentration of MDA was estimated and expressed as nmol MDA per 10^6 cells.

Text S11. Soluble EPS and P/C ratio measurement

Soluble Extracellular polymeric substances (EPS) produced during the exposure period were analyzed at 24, 48, and 72 hours according to previously published protocol with modification [11]. Briefly, 15 mL of culture from each treatment flask was collected at the end of each time point, and the cells were centrifuged at 8500 g for 15 minutes. The supernatant was carefully removed and filtered through a 0.25 μm filter to eliminate any residual debris. The soluble EPS was quantified as dissolved organic carbon (DOC) using a TOC analyzer (Model TOC-L, Shimadzu). Additionally, the protein content of the soluble EPS was measured using the BSA assay [12] (BioRad laboratories, US), and the carbohydrate content was determined using the phenol-sulphuric acid assay [13] (Sigma Aldrich, US). These additional assays provided a detailed profile of the EPS composition by allowing the quantification of both protein and carbohydrate components, thereby offering insights into the biochemical characteristics of the substances produced under each treatment condition.

Text S12. FTIR Analysis

To examine changes in the surface chemistry of microalgal cells upon NPl exposure, ATR-FTIR analysis was performed. At the end of the exposure test, the culture solution from each treatment was washed with 10× PBS at least three times to remove any loosely bound NPls. After washing, the cells were lyophilized at –55 °C for 72 hours. The dried, lyophilized cells were then mounted for ATR-FTIR analysis using a PerkinElmer Inc. instrument (UK), scanning spectra from 4000 to 400 cm^{-1} with a data interval of 1 cm^{-1} and a resolution of 4 cm^{-1}. Additionally, dried NPls were examined to compare any alterations in the surface chemistry of the microalgae exposed to NPls.

Text S13. Morphological observations via SEM

To visualize changes in the surface morphology of microalgal cells, scanning electron microscopy (SEM) were employed. At the end of the exposure period, cells from each treatment were collected and washed three times with 1× PBS. The cells were then fixed in a 2.5% (v/v) glutaraldehyde solution in 10× PBS at 4 °C for 24 hours. After fixation, the cells were washed again with 1× PBS and dehydrated using a graded series of ethanol solutions (60%, 70%, 80%, 90%, and 100%). The dehydrated cells were mounted on carbon tape, air-dried, and coated with gold before being examined using a ZEISS EVO 10 SEM at 20 kV.

Table S1. Chemical composition of Bold Basal's Media (BBM)

No.	Compound	Chemical Formula	Concentration (g/L)
1	Potassium di-hydrogen orthophosphate	KH_2PO_4	17.50
2	di-Potassium hydrogen orthophosphate	K_2HPO_4	7.50
3	Magnesium sulphate	$MgSO_4 \cdot 7H_2O$	7.50
4	Sodium nitrate	$NaNO_3$	25.00
5	Calcium chloride	$CaCl_2 \cdot 2H_2O$	2.50
6	Sodium chloride	NaCl	2.50
7	EDTA tetrasodium salt	$EDTA–Na_4$	50.0
	+ Potassium hydroxide	KOH	31.0
8	Ferrous sulphate	$FeSO_4 \cdot 7H_2O$	4.98
	+ Conc. Sulphuric acid	H_2SO_4	10ml/L
9	Boric acid	H_3BO_3	1.142
10	Zinc sulphate	$ZnSO_4 \cdot 7H_2O$	14.12
11	Manganese chloride	$MnCl_2 \cdot 4H_2O$	2.32
12	Copper sulphate	$CuSO_4 \cdot 5H_2O$	2.52
13	Cobaltous nitrate	$Co(No_3)_2 \cdot 6H_2O$	0.80
14	Sodium molybdate	$Na_2MoO_4 \cdot 2H_2O$	1.92

Table S2. ICP-MS operational parameters

Parameter/Component	
Nebulizer	MEINHARD HEN
Nebulizer gas flow	1.1 L/min
Spray Chamber	Glass cyclonic
RF Power	1600 W

Table S3. Single-cell ICP-MS operational parameters NexION 300D

Single-cell ICP-MS parameters	
Radio frequency power	1600 W
Nebulizer type	MEINHARD HEN
Spray chamber type	Asperon
Plasma gas flow	15 L/min
Nebulizer gas flow	0.5 L/min
Auxiliary gas flow	1.2 L/min
Sample flow rate	0.01 ml/min
Transport efficiency	10.9%
Dwell time	40 µs
Acquisition time	50 s

Table S4. Theoretical calculations of Eu loading per particle

Eu-doped NPls Concentration (mg/L)	**Particle Concentration (Part/L)**	**Eu mass (µg/L)**	**Eu content (µg Eu/mg NPls)**	**Estimated Eu loading (ag/part)**
5	3.69924E+11		0.854	11.549
5	3.94072E+11	4.272	0.854	10.841
5	3.52883E+11		0.854	12.107
10	7.9945E+11		0.796	9.952
10	4.44525E+11	7.956	0.796	17.898
10	6.21988E+11		0.796	12.926
20	1.32899E+12		0.939	14.132
20	1.76193E+12	18.782	0.939	10.660
20	1.09367E+12		0.939	17.173
		Average	**0.86 ± 0.06**	**13.02 ± 2.68**

Table S5. Recovery rate of Eu-doped NPls during exposure test

Exposure (mg/L)	Time (h)	Dry weight mg/mL	Total Biomass mg in system*	Eu-doped NPls in Pellet (µg/mg biomass)	Eu-doped NPls in SN (mg/L)*	SN Recovery (%)	Pellet Recovery (%)	Total Recovery (%)
5	24	0.75	187.16	3.76	2.36	47.2	56.3	103.5
5	48	0.77	193.49	3.54	1.48	29.7	54.7	84.4
5	72	0.89	221.29	3.54	2.95	59	62.6	121.6
10	24	0.75	187.07	5.32	6.20	62	39.9	101.9
10	48	0.77	191.47	4.61	7.69	76.9	35.3	112.2
10	72	0.88	219.13	4.57	5.40	54	40	94
20	24	0.75	186.89	5.70	14.58	72.9	21.4	94.2
20	48	0.76	190.43	5.42	17.00	85	20.6	105.6
20	72	0.86	214.53	5.22	14.23	71.1	22.5	93.6

**Working volume=250 mL; SN=Supernatant*

Table S6. GMM Table Summary

Group	Cluster 1			Cluster 2			Cluster 3			Cluster 4			Cluster 5			*MAE*	*RMSE*	*ρ*
	γ1	*μ1*	*σ1*	*γ2*	*μ2*	*σ3*	*γ3*	*μ3*	*σ3*	*γ4*	*μ4*	*σ4*	*γ5*	*μ5*	*σ5*			
5 mg/L (24 h)	0.5544	62.49	16.55	0.399	320.08	146.06	0.0466	1175.78	360.72	-	-	-	-	-	-	59.18	108.85	0.935
5 mg/L (48 h)	0.3365	66.1	6.67	0.4408	128.48	35.83	0.2085	405.5	147.35	0.0142	2649.67	1418.11	-	-	-	49.38	143.82	0.922
5 mg/L (72 h)	0.5255	62.55	17.21	0.382	154.02	45.58	0.0925	391.54	164.86	-	-	-	-	-	-	25.47	58.89	0.893
10 mg/L (24 h)	0.6292	47.64	9.53	0.2772	78.95	29.29	0.0936	306	120.66	-	-	-	-	-	-	19.11	37.45	0.905
10 mg/L (48 h)	0.0672	65.39	21.32	0.3599	208.62	80.18	0.5729	662.44	286.64	-	-	-	-	-	-	36.68	86.09	0.906
10 mg/L (72 h)	0.09	91.7	19.55	0.2655	169.74	28.56	0.2938	326.69	71.66	0.3507	637.82	167.36	-	-	-	36.08	68.2	0.953
20 mg/L (24 h)	0.1962	69.07	4.89	0.4753	109.81	29.52	0.2061	215.06	39.24	0.0987	434.47	107.06	0.0237	1188.23	461.52	25.28	80.02	0.942
20 mg/L (48 h)	0.6442	59.23	17.35	0.2907	152.46	48.51	0.0651	480.01	246.47	-	-	-	-	-	-	24.16	65.8	0.883
20 mg/L (72 h)	0.4091	201.07	43.42	0.3863	418.25	99.77	0.2046	968.81	322.74	-	-	-	-	-	-	77.41	157.11	0.919

Table S7. Approximate nanoplastic particle equivalents associated with C. vulgaris subpopulations identified by Gaussian mixture modelling of SC-ICP-MS data. Values represent approximate association burdens rather than exact particle counts.

Cluster/Subpopulation	Eu mass per cell (ag)	Approx. NPl particle equivalents per cell	Conservative interpretation
1	45–80	3–6	very low associated burden
2	80–220	6-17	low associated burden
3	220-500	17-38	moderate associated burden
4	500-1200	38-92	high associated burden
5	1200-2700	92-205	very high associated burden

Table S8. Reduced GLM pairwise Table Summary

Term	Estimate	SE	statistic	p.value	Cluster_Pair	AIC	RMSE	McFadden_R^2	Nagelkerke_R^2
(Intercept)	0.619	15.818	0.039	0.971	cluster1 + cluster2	62.19929	3.935	0.907172	0.9074906
dose_mgL	0.867	0.316	2.747	0.052					
time_h	0.528	0.108	4.903	0.008					
cluster1	-0.095	9.916	-0.010	0.993					
cluster2	-30.420	30.339	-1.003	0.373					
(Intercept)	-30.855	9.945	-3.103	0.036	cluster1 + cluster3	56.88105	2.928391	0.94859	0.9489231
dose_mgL	0.893	0.235	3.800	0.019					
time_h	0.552	0.077	7.192	0.002					
cluster1	27.984	13.398	2.089	0.105					
cluster3	41.213	18.362	2.245	0.088					
(Intercept)	-11.349	8.935	-1.270	0.273	Cluster1 + cluster4	63.29992	4.18312	0.8950965	0.8954108
dose_mgL	0.876	0.336	2.611	0.059					
time_h	0.576	0.113	5.121	0.007					
cluster1	-1.916	12.212	-0.157	0.883					
cluster4	-15.732	24.013	-0.655	0.548					
(Intercept)	-5.715	7.507	-0.761	0.489	cluster1 + cluster5	58.29271	3.167298	0.9398595	0.9401895
dose_mgL	1.222	0.311	3.922	0.017					
time_h	0.432	0.106	4.079	0.015					
cluster1	-6.884	9.111	-0.756	0.492					
cluster5	-632.434	327.64	-1.930	0.126					
(Intercept)	0.120	12.485	0.010	0.993	cluster2 + cluster3	60.83065	3.646893	0.9202675	0.9205907
dose_mgL	0.866	0.292	2.961	0.042					
time_h	0.510	0.098	5.194	0.007					
cluster2	-32.118	27.222	-1.180	0.303					
cluster3	9.884	12.193	0.811	0.463					
(Intercept)	3.378	11.665	0.290	0.787		59.27041	3.344093	0.9329581	0.9332857

dose_mgL	0.875	0.268	3.261	0.031	cluster2 + cluster4			
time_h	0.558	0.091	6.144	0.004				
cluster2	-39.254	25.898	-1.516	0.204				
cluster4	-20.644	16.643	-1.240	0.283				
(Intercept)	-7.694	13.423	-0.573	0.597	cluster2 + cluster5	59.42837	3.373568	0.9317711	0.9320983
dose_mgL	1.130	0.348	3.249	0.031				
time_h	0.473	0.100	4.747	0.009				
cluster2	-5.531	32.511	-0.170	0.873				
cluster5	-458.889	382.10	-1.201	0.296				
(Intercept)	-13.580	6.545	-2.075	0.107	cluster3 + cluster4	61.98468	3.888364	0.9093593	0.9096786
dose_mgL	0.877	0.312	2.811	0.048				
time_h	0.564	0.106	5.332	0.006				
cluster3	10.668	13.153	0.811	0.463				
cluster4	-16.267	18.871	-0.862	0.437				
(Intercept)	-10.946	4.904	-2.232	0.089	cluster3 + cluster5	56.71209	2.901031	0.9495462	0.9498796
dose_mgL	1.178	0.274	4.300	0.013				
time_h	0.444	0.088	5.044	0.007				
cluster3	11.761	9.773	1.203	0.295				
cluster5	-545.257	256.440	-2.126	0.101				
(Intercept)	-10.020	5.686	-1.762	0.153	cluster4 + cluster5	59.38257	3.364995	0.9321174	0.9324447
dose_mgL	1.140	0.323	3.535	0.024				
time_h	0.482	0.111	4.360	0.012				
cluster4	-3.866	17.378	-0.222	0.835				
cluster5	-473.490	317.821	-1.490	0.211				

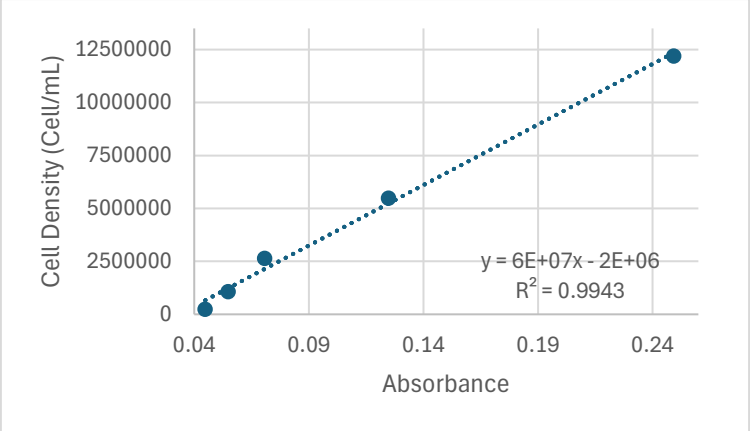

Figure S1. Linear Correlation Curve of Cell Density (Counting Chamber) and Optical Density (Uv-Vis Spectrophotometry)

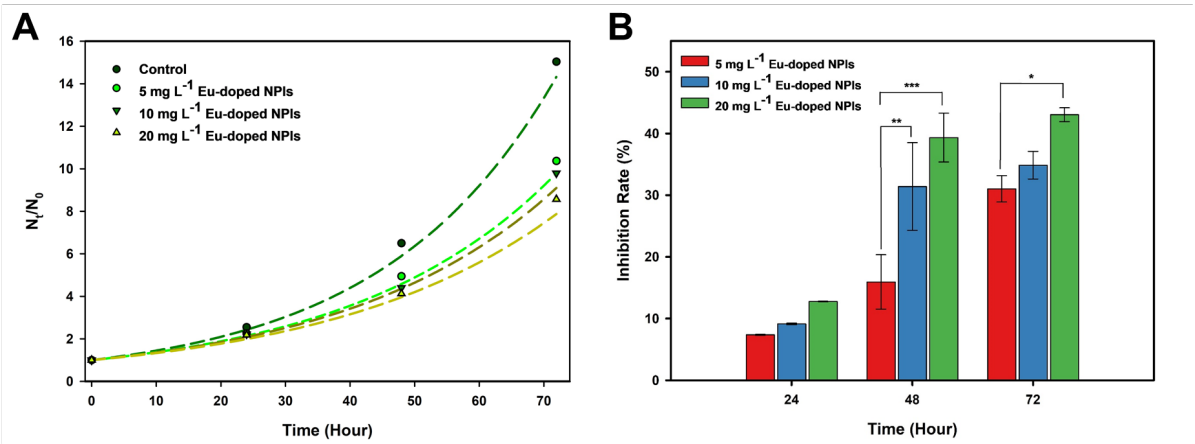

Figure S2. Observation of growth during 72 h growth inhibition test. (A) Growth rate of control and Eu-doped NPls exposed cells, dashed line represents first order nonlinear growth rate model. (B) Growth Inhibition Rate (IR) of C. vulgaris exposed to 5, 10 and 20 mg/L in relative to control (Line depicting significance level between concentration). Plot graphs represent mean ± SD (n = 3) and bars with an asterisk indicates statistically significant difference (* = $p < 0.05$, ** = $p < 0.01$, *** = $p < 0.001$) when compared to control using one-way ANOVA.

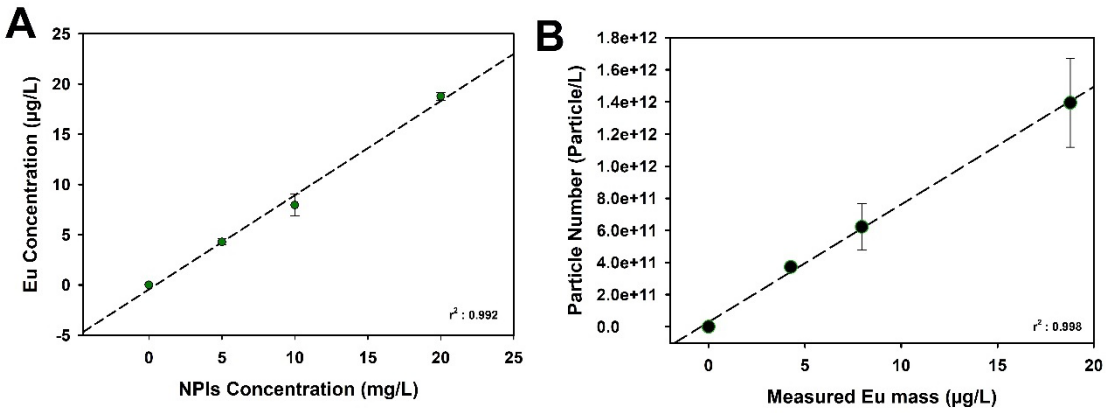

Figure S3. Calibration relationship between Eu signal and Eu-doped nanoplastic concentration. (A) Measured Eu concentration (µg/L) as a function of nominal Eu-doped NPls concentration (mg/L) following complete digestion and ICP-MS quantification (r^2 = 0.992). (B) Linear correlation between measured Eu mass (µg/L) and particle number concentration determined by SP-ICP-MS for the same Eu-doped NPl suspensions (r^2 = 0.998). Dashed lines indicate linear regression fits and error bars represent standard deviations of replicate measurements (n=3).

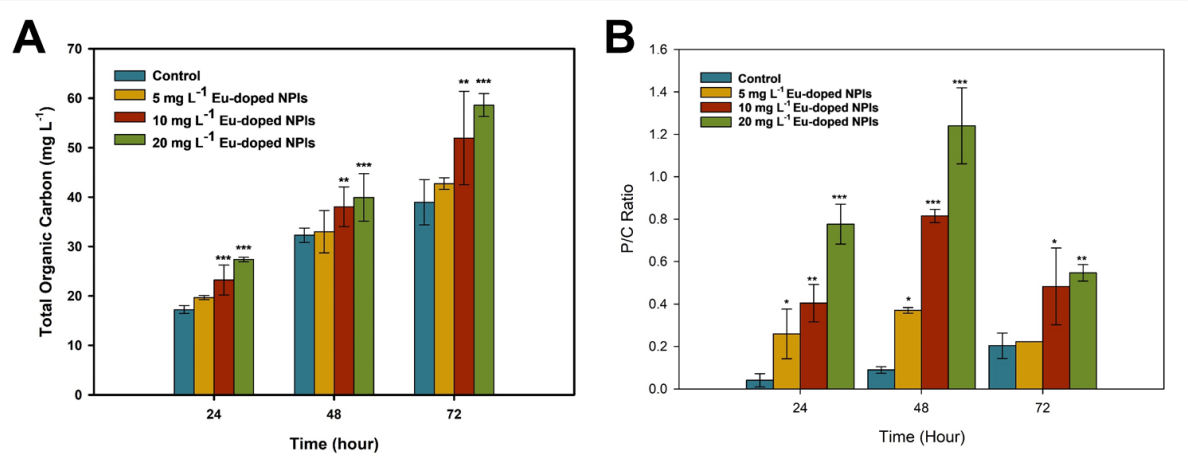

Figure S4. Exopolysaccharide produced during 72 h growth inhibition test. (A) Soluble EPS production expressed by dissolved organic carbon (DOC) and (B) protein-to-carbohydrate (P/C) ratio recorded daily during exposure test. Plot graphs represent mean ± SD (n = 3). Bars with an asterisk indicate statistically significant differences (* = $p < 0.05$, ** = $p < 0.01$, *** = $p < 0.001$) when compared to control using Kruskal-Wallis test.

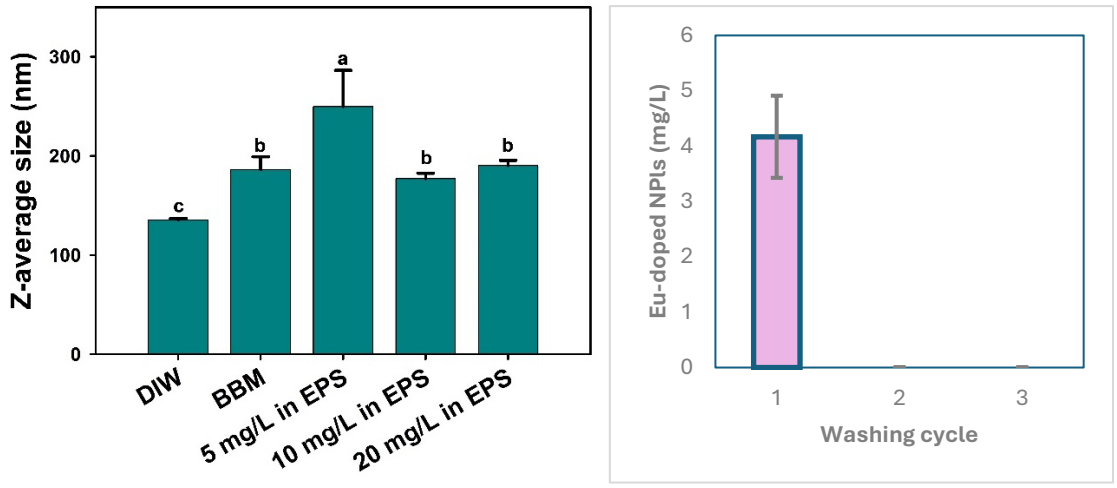

Figure S5. (A) Z-average size of Eu-doped NPls after 24 h incubated in cell-free EPS medium, indicating EPS-induced aggregation. Alphabetical notation showing significant different of One-way ANOVA followed by Holm-sidak test, different notation indicates statistically significant different at $p>0.05$. (B) Sequential washing efficiency for removal of loosely associated Eu-doped NPls. Eu-doped NPls detected in supernatants from three PBS washing cycles for a representative exposure (20 mg/L, 72 h). Each wash used 20 mL 10× PBS followed by centrifugation at 3600 g for 10 min. Supernatants were collected, digested, and analysed for Eu by ICP-MS, with concentrations converted to Eu-doped NPl mass. Most particles were removed during the first wash, with negligible amounts detected in subsequent washes.

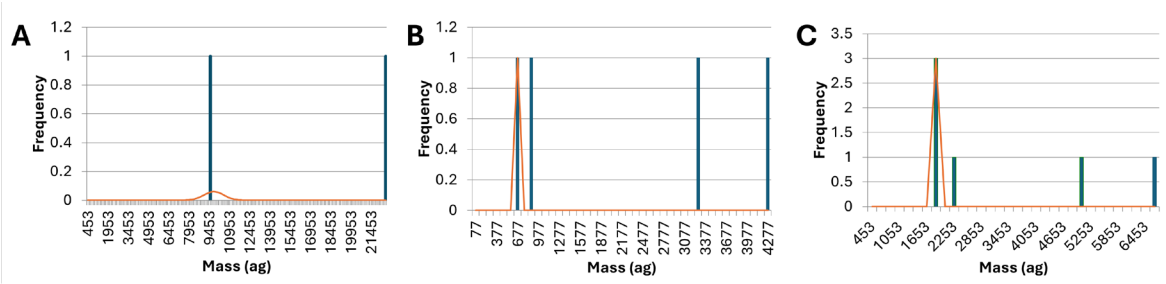

Figure S6. Representative SC-ICP-MS mass distributions obtained for control Eu-doped NPls dispersed in DIW at nominal concentrations of (A) 5 mg/L, (B) 10 mg/L, and (C) 20 mg/L. All scans were acquired under identical acquisition conditions with a 50 s acquisition time. Only a limited number of detectable events were observed, suggesting that individual NPls are generally below the SC-ICP-MS detection limit, while occasional signals likely correspond to particle aggregates or clusters exceeding the mass detection threshold.

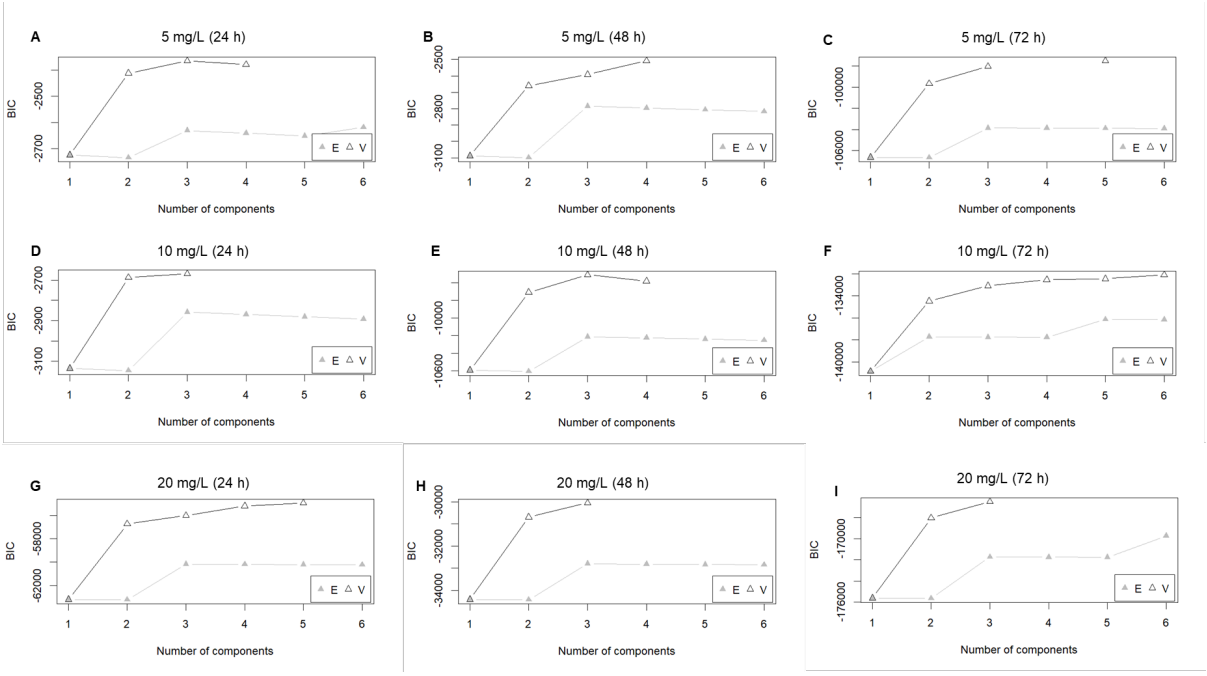

Figure S7. Model selection for Gaussian Mixture Models (GMM) across different exposure conditions. Bayesian Information Criterion (BIC) values plotted against the number of GMM components (1–6) for three Eu concentrations (5, 10, and 20 mg/L) and three time points (24, 48, and 72 h). Each curve represents a different covariance structure: Equal (E, △), Diagonal (△, ▽), and Varying (V, ◯).

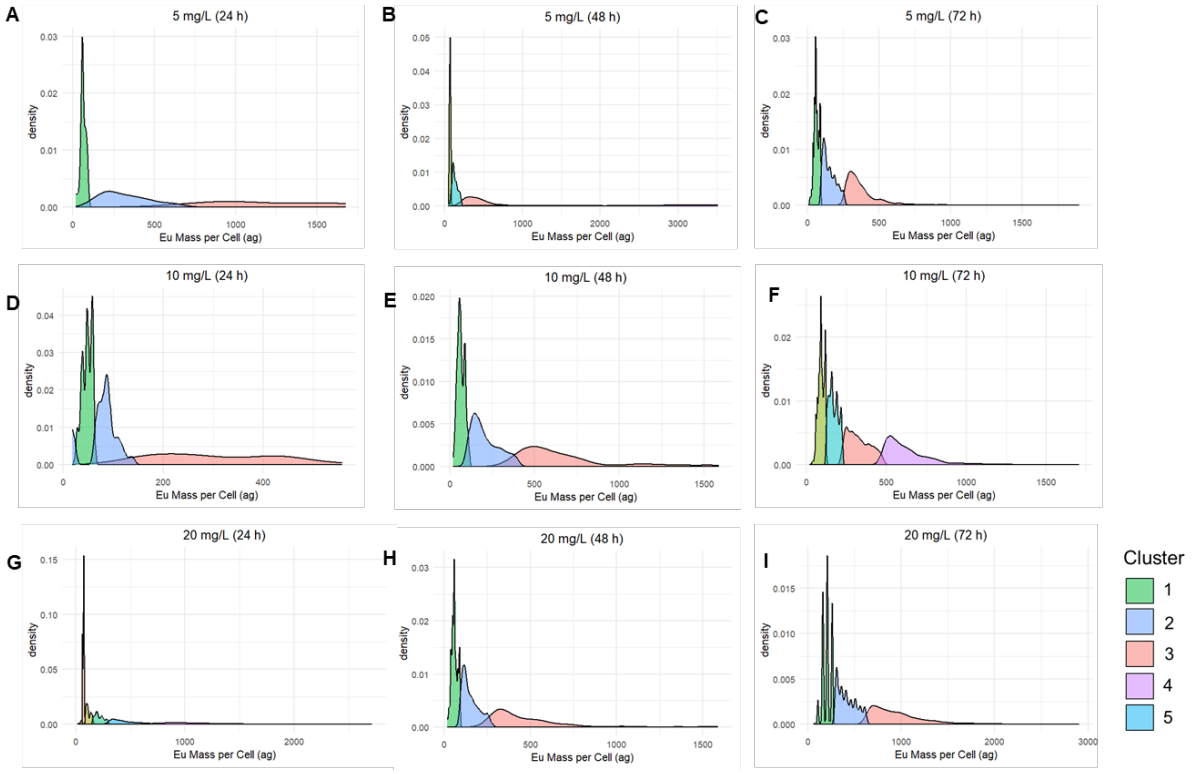

Figure S8. Density distributions of Eu mass per cell fitted with GMM components across exposure conditions. Kernel density plots showing Eu mass per cell (ag) distributions for individual cells exposed to 5, 10, or 20 mg/L Eu for 24, 48, or 72 h. Coloured areas indicate GMM-derived clusters representing different levels of cellular association

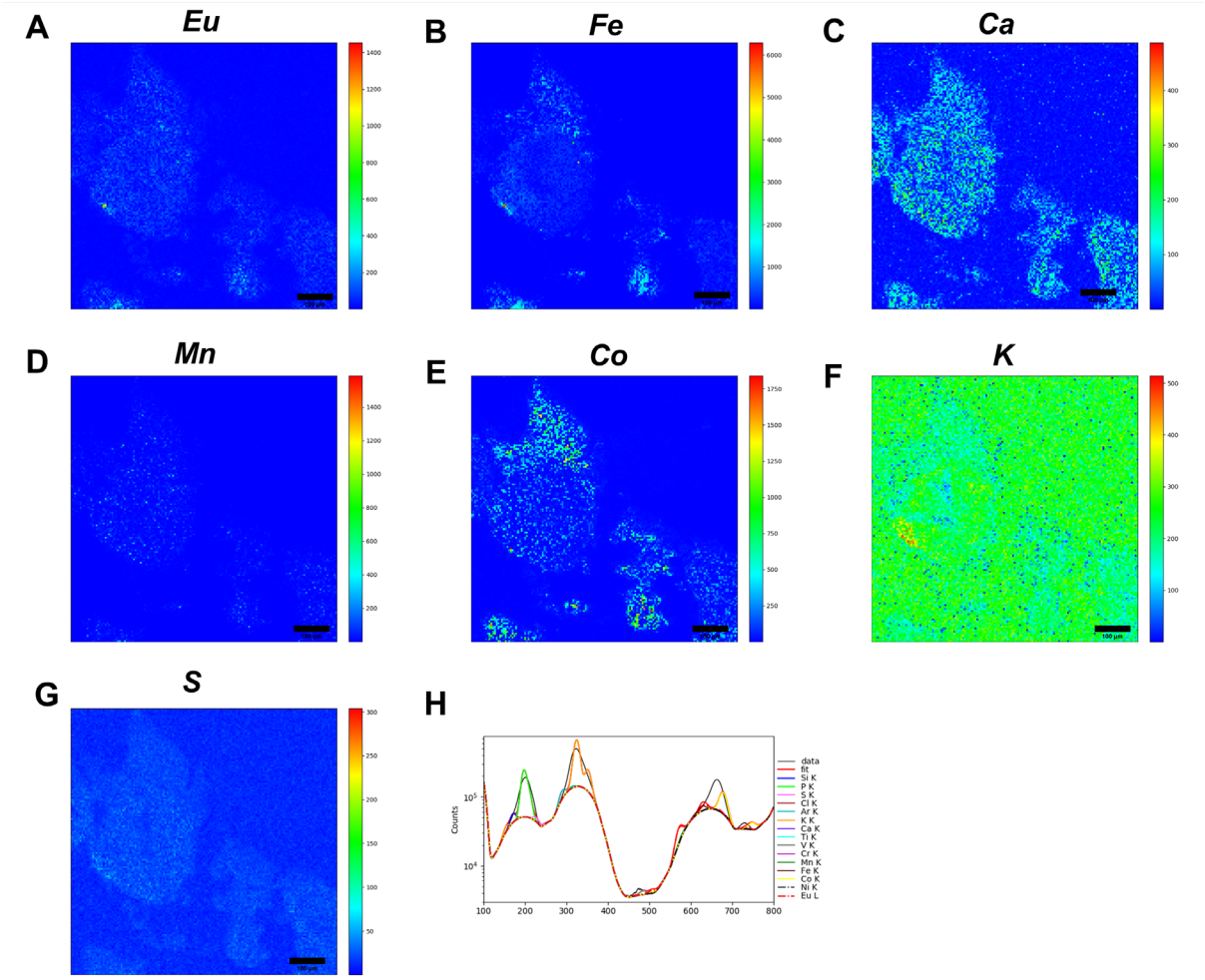

Figure S9. Synchrotron-based X-ray fluorescence (XRF) elemental mapping of untreated *Chlorella vulgaris* cells (control). Distribution maps are shown for (A) Eu, (B) Fe, (C) Ca, (D) Mn, (E) Co, (F) K, and (G) S. The colour scale indicates relative fluorescence intensity, with blue representing low and red representing high signal intensity. (H) Representative XRF spectrum confirming elemental signals detected in the control sample fitted with PyMca.

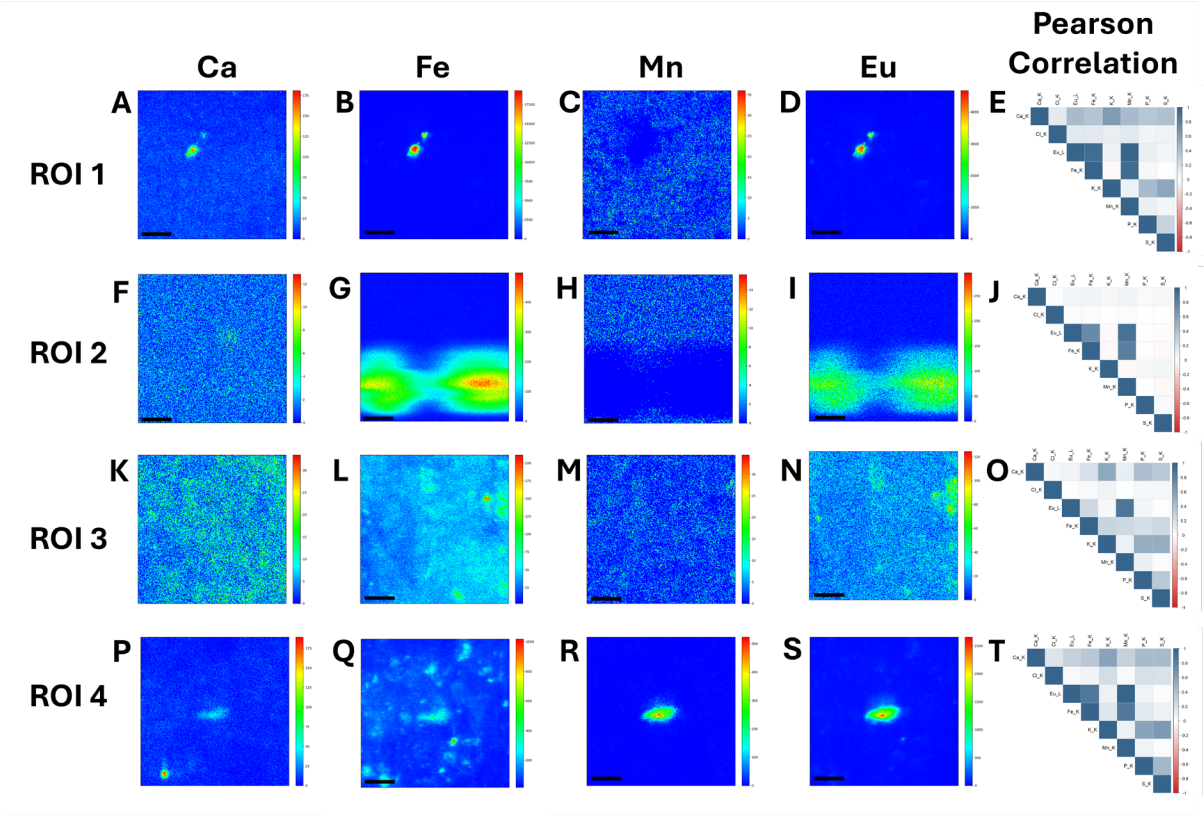

Figure S10. Additional synchrotron nano-XRF elemental maps from four representative regions of interest (ROI 1–4) of Chlorella vulgaris cells exposed to Eu-doped NPls (10 mg/L). Elemental distributions of Ca, Fe, Mn, and Eu are shown for each ROI, together with corresponding pixel-wise Pearson correlation matrices calculated from the XRF intensity maps. Each ROI corresponds to a 10 × 10 µm scan area acquired with a 50 nm step size. The scale bar represents 2 µm. The maps illustrate variability in the spatial relationships between Eu hotspots and intracellular elements across different regions. Pearson correlation values reflect overall pixel-intensity relationships within each ROI and should therefore be interpreted cautiously, as correlations can be influenced by shared background signals and the two-dimensional projected nature of nano-XRF imaging.

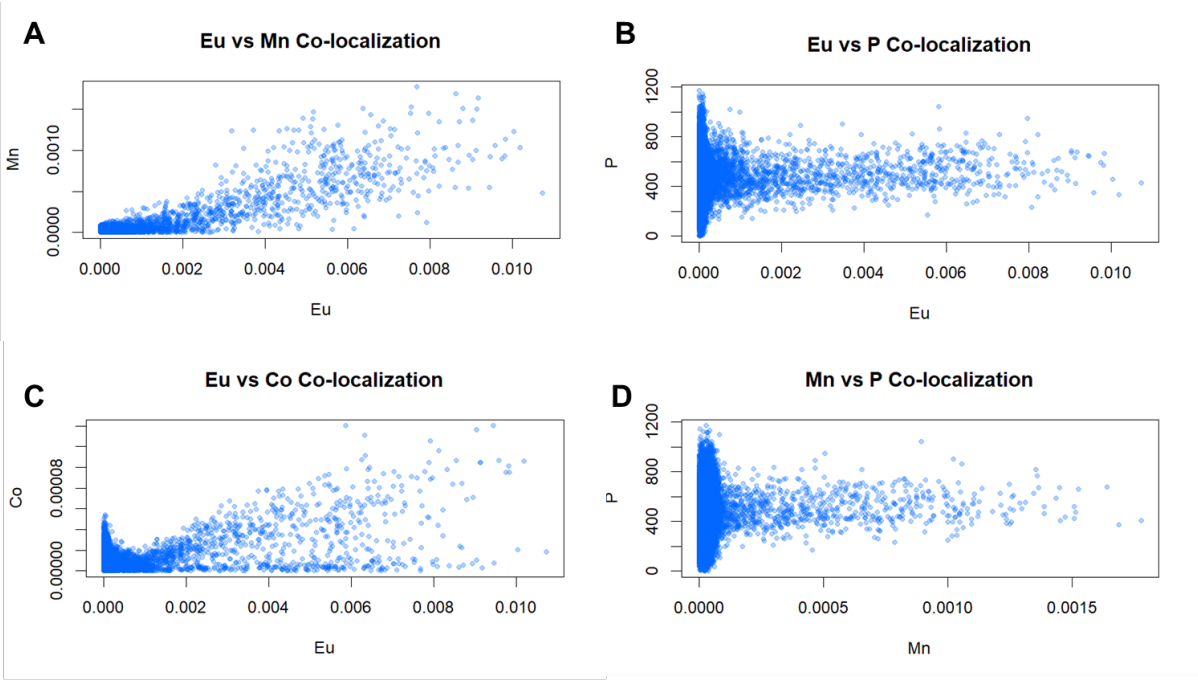

Figure S11. Pixel-by-pixel Co-localization analysis of (A) Eu and Mn, (B) Eu and P, (C) Eu and Co, (D) Mn and P.

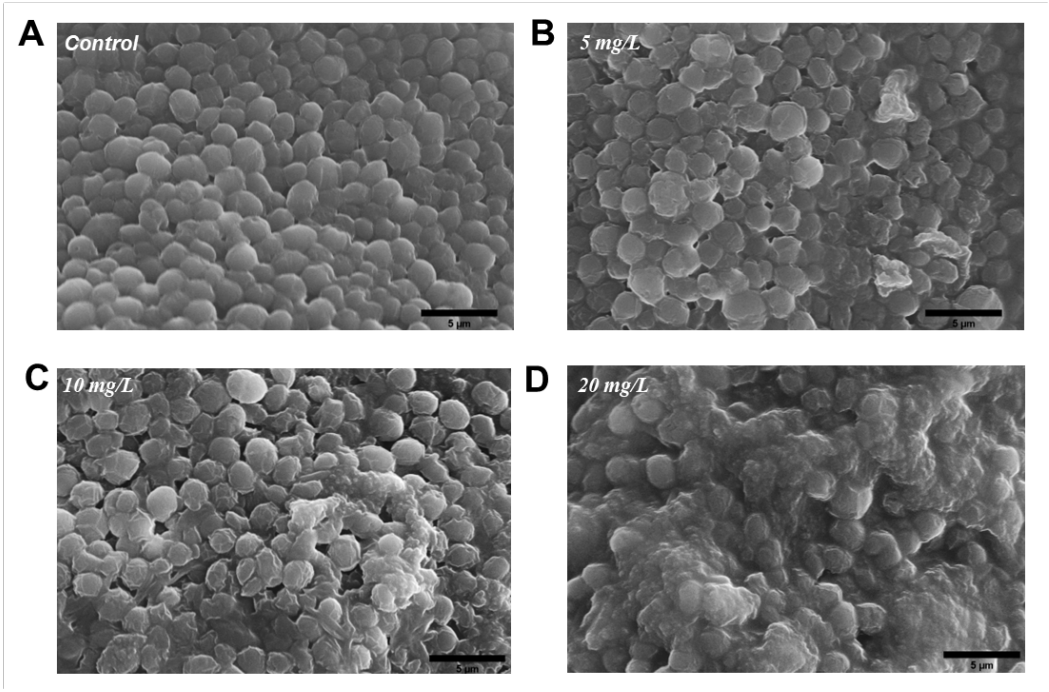

Figure S12. Scanning Electron Microscopy (SEM) images showing surface morphology of microalgae: (A) control (no Eu-doped NPls), (B) treated with 5 mg/L Eu-doped NPls and (C) 10 mg/L Eu-doped NPls, and (D) treated with 20 mg/L Eu-doped NPls.

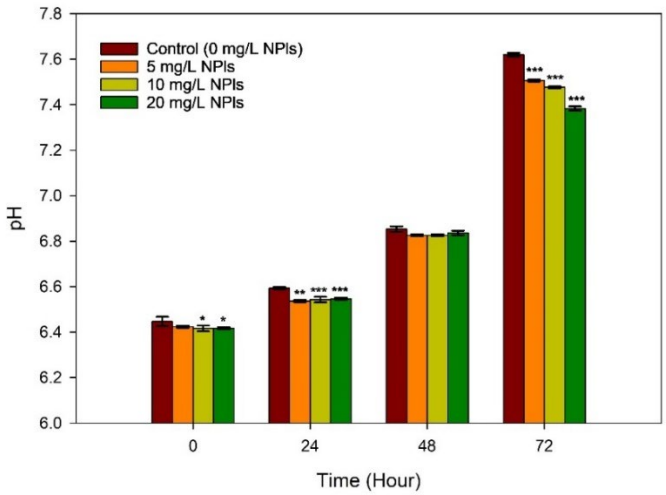

Figure S13. Changes of pH across treatment during 72 h growth inhibition test. Bars with an asterisk indicate statistically significant differences (* = $p < 0.05$, ** = $p < 0.01$, *** = $p < 0.001$) when compared to control using Kruskal-Wallis test.

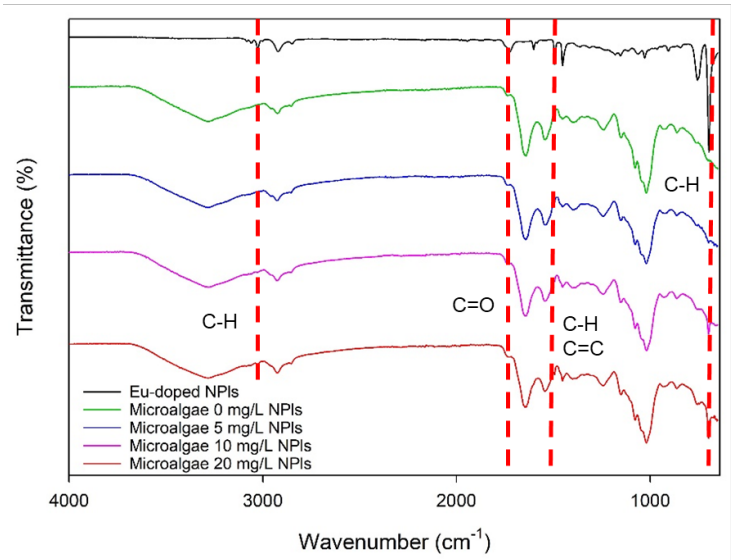

Wavenumber (cm^{-1})	Association
700	out-of-plane bending vibrations of aromatic C–H bonds
760	out-of-plane bending vibrations of C–H bonds in aromatic rings.
1492	C=C stretching vibrations in aromatic rings.
1450	C–H bending (or scissoring) vibrations in $-CH_2$ and $-CH_3$ groups.
1720	C=O stretching vibration of Carbonyl group
3000	C–H stretching vibrations

Figure S14. FTIR spectra of cells unexposed and exposed to NPls after 72 h and the assigned peaks

References

[1] J.C. Achar, J.-H. Kwon, J. Jung, Toxicokinetic modeling of octylphenol bioconcentration in Chlorella vulgaris and its trophic transfer to Daphnia magna, Ecotoxicology and Environmental Safety, 194 (2020) 110379.
[2] W. Yang, P. Gao, H. Li, J. Huang, Y. Zhang, H. Ding, W. Zhang, Mechanism of the inhibition and detoxification effects of the interaction between nanoplastics and microalgae Chlorella pyrenoidosa, Science of the Total Environment, 783 (2021) 146919.
[3] S. Meyer, A. López-Serrano, H. Mitze, N. Jakubowski, T. Schwerdtle, Single-cell analysis by ICP-MS/MS as a fast tool for cellular bioavailability studies of arsenite, Metallomics, 10 (2018) 73-76.
[4] Y. Li, X. Wang, D. Liang, X. Zhao, Z. Dong, Y. Bai, W.-X. Wang, W.J. Peijnenburg, Y. Wang, W. Fan, Modelling the size distribution and bioaccumulation of gold nanoparticles under mixture exposure, Aquatic Toxicology, (2025) 107286.
[5] H. Chen, L. Wang, B. Hu, J. Xu, X. Liu, Potential driving forces and probabilistic health risks of heavy metal accumulation in the soils from an e-waste area, southeast China, Chemosphere, 289 (2022) 133182.
[6] S. Tang, Y. Liu, J. Zhu, X. Cheng, L. Liu, K. Hammerschmidt, J. Zhou, Z. Cai, Bet hedging in a unicellular microalga, Nature Communications, 15 (2024) 2063.
[7] Z. Sun, S. Zhang, T. Zheng, C. He, J. Xu, D. Lin, L. Zhang, Nanoplastics inhibit carbon fixation in algae: The effect of aging, Heliyon, 10 (2024).
[8] L.J. Hazeem, G. Kuku, E. Dewailly, C. Slomianny, A. Barras, A. Hamdi, R. Boukherroub, M. Culha, M. Bououdina, Toxicity effect of silver nanoparticles on photosynthetic pigment content, growth, ROS production and ultrastructural changes of microalgae Chlorella vulgaris, Nanomaterials, 9 (2019) 914.

[9] P. Singh, S. Singh, P. Maurya, A. Mohanta, H. Dubey, S.R. Khadim, A.K. Singh, A.K. Pandey, A.K. Singh, R.K. Asthana, Bioaccumulation of selenium in halotolerant microalga Dunaliella salina and its impact on photosynthesis, reactive oxygen species, antioxidative enzymes, and neutral lipids, Marine Pollution Bulletin, 190 (2023) 114842.
[10] S. Gaweł, M. Wardas, E. Niedworok, P. Wardas, Malondialdehyde (MDA) as a lipid peroxidation marker, Wiadomosci lekarskie (Warsaw, Poland: 1960), 57 (2004) 453-455.
[11] S. Giri, A. Mukherjee, Ageing with algal EPS reduces the toxic effects of polystyrene nanoplastics in freshwater microalgae Scenedesmus obliquus, Journal of Environmental Chemical Engineering, 9 (2021) 105978.
[12] J. Thabet, J. Elleuch, F. Martínez, S. Abdelkafi, L.E. Hernández, I. Fendri, Characterization of cellular toxicity induced by sub-lethal inorganic mercury in the marine microalgae Chlorococcum dorsiventrale isolated from a metal-polluted coastal site, Chemosphere, 338 (2023) 139391.
[13] T. Masuko, A. Minami, N. Iwasaki, T. Majima, S.-I. Nishimura, Y.C. Lee, Carbohydrate analysis by a phenol–sulfuric acid method in microplate format, Analytical Biochemistry, 339 (2005) 69-72.